Escape-time model for the current self-oscillation frequencies in weakly coupled semiconductor superlattices

M. Rogozia, H. T. Grahn, and R. Hey
Paul-Drude-Institut für Festkörperelektronik, Hausvogteiplatz 5–7, 10117 Berlin, Germany

Abstract: A semiclassical model was developed to predict the frequencies of current self-oscillations in weakly coupled semiconductor superlattices (SLs). The calculated frequency is derived from the escape time out of the well and the tunneling probability through the barrier, using the well and barrier width, effective masses and band offsets as well as the resulting energies of the sub- and minibands as input parameters. For all SLs, the measured frequency dependence on the sample parameters can be well described by our model. For weakly (strongly) coupled SLs, the calculated frequencies are somewhat above (below) the observed ones. The changeover from one to the other behavior occurs for SLs with miniband widths of a few meV.

1. Introduction

Self-oscillations of the current have been observed in doped, weakly coupled [1-4] and strongly coupled semiconductor superlattices (SLs) [5-7] as well as in undoped, photoexcited ones [8-10]. The SLs can be divided into two groups according to the dominant transport mechanism along the SL axis. Strongly coupled SLs exhibit a large width of the lowest subband relative to the level broadening due to scattering effects, typically of the order of a few meV. In this case, the transport is referred to as miniband transport. However, in weakly coupled SLs, the width of the lowest subband is smaller than the level broadening. Therefore, the carriers can only tunnel sequentially from the first subband of one well to the first or a higher subband in the adjacent well. This process is called sequential resonant tunneling.

For doped, weakly coupled SLs, frequencies from below 1 MHz up to 10 GHz have been reported [1-4]. In this case, the current self-oscillations are caused by a recycling motion of a charge monopole, which forms the boundary between a low- and a high-field domain [11, 12]. The oscillation of the domain boundary is confined to 30–40% of the total length of the SL [2]. In contrast to weakly coupled SLs, the mode of the current self-oscillations in strongly coupled SLs is very similar to the one present in the Gunn effect [13], i.e., a propagating dipole domain [14] traversing the whole length of the SL. The observed frequencies vary from a few GHz up to more than 100 GHz [5-7].

We present a simple model to predict the oscillation frequency for weakly coupled SLs using the sample parameters well and barrier width, effective masses, band offset between well and barrier material, and the resulting energies of the involved subbands. The increase of the frequencies with decreasing barrier width and effective barrier height can be very well predicted. This model has been developed, since microscopic theoretical transport models usually predict a frequency more than one order of magnitude below the experimentally observed one.

2. Experiment

The SL parameters well width d_W and barrier width d_B are listed in Table 1. The samples are GaAs/AlAs SLs grown on GaAs substrates except for the $d_W/d_B = 10.0/4.0$ sample, which is an In(Ga,As)/(In,Al)As SL grown lattice matched on InP. The SLs are moderately doped in the center of each well with a typical doping level in the 10^{16} cm^{-3} range. The SLs are embedded between highly doped GaAs or $Al_{0.5}Ga_{0.5}As$ contact layers. After the growth by molecular beam epitaxy (MBE), the samples are etched into mesas with diameters between 16 and 200 μm and provided with Ohmic contacts.

For the experiments, several mesas are mounted on a sapphire sample holder with gold stripes and put into a He flow cryostat. At the back contact, the DC voltage is applied through a bias-tee. The top contact is connected to a spectrum analyzer (Advantest R3272 or R3361A) or a sampling oscilloscope (Tektronix CSA 803) with an input impedance of 50 Ω to measure the frequency (power) spectrum or

Tab. 1 Sample parameters and oscillation frequencies for weakly coupled SLs. d_W denotes the well width, d_B the barrier width, N the number of SL periods, i the index of the corresponding plateau of the I-V characteristic, E_i the energy and Δ_i the width of the i^{th} sub- or miniband, and f_i the measured oscillation frequency. The symbols are used in Figs. 3 and 4 to distinguish different samples. Solid symbols refer to weakly, open symbols to more strongly coupled SLs. Except for the 10.0/4.0 sample (✳), which is an (In,Ga)As/(In,Al)As SL grown lattice matched on InP, all other SLs are GaAs/AlAs.

d_W (nm)	d_B (nm)	N	symbol	i	E_i (meV)	Δ_i (meV)	f_i (MHz)
9.0	1.4	40	□	1	44.3	4.5	5,000
9.0	1.5	40	◇	1	44.5	3.7	1,500
15.0	0.9	40	△	1	18.6	3.7	2,500
10.1	1.4	40	▽	1	36.7	3.4	1,800
10.0	4.0	40	✳	1	48.0	2.0	1,800
15.0	1.7	40	●	1	18.8	0.7	500
				2	75.8	2.8	8,000
20.0	2.0	40	♦	1	11.3	0.2	—
				2	45.3	0.7	600
				3	102.2	1.7	1,200
				4	182.4	3.2	2,300
13.3	2.7	50	▼	1	23.3	0.1	25
				2	93.0	0.6	500
				3	211.0	1.6	1,200
15.0	2.9	40	▲	1	19.0	< 0.1	45
				2	75.8	0.3	500
				3	171	0.8	1,700
				4	305	1.9	4,000
9.0	4.0	40	■	1	44.4	< 0.1	1
				2	180.0	0.1	20

the time trace, respectively, of the self-sustained current oscillations. A detailed schematic diagram of the experimental setup is shown in Fig. 1.

3. Escape time model

From Table 1, in particular for the set of samples with a constant well width of 15 nm and different barrier widths (0.9, 1.7, 2.9 nm), it appears that the frequency of the current self-oscillations depends exponentially on the barrier width. The simplest approach to obtain such a frequency dependence is to consider the coupling between different wells in the Wentzel-Kramers-Brillouin (WKB) approximation. In this case, the dominant term determining the tunneling probability $T(E_i)$ between adjacent wells is given by

$$T(E_i) = \exp\left(-\frac{2d_B}{\hbar}\sqrt{2m_B^*(V_0 - E_i)}\right) , \tag{1}$$

where m_B^* denotes the effective electron mass in the barrier and V_0 the conduction band offset between well and barrier material. The difference $V_0 - E_i$ is a measure for the effective barrier height, which decreases with increasing electric field. We used this very simple model previously to demonstrate that the frequency dependence of the current oscillations in weakly coupled SLs is dominated by the exponential dependence on the barrier width as well as on the effective barrier height [4].

In order to calculate not only the tunneling probability, but also the frequency of the current oscillations, we introduce the classical round trip time τ_{rt} for an electron in a potential well of width d_W

$$\tau_{rt}(E_1) = \frac{2\,d_W}{v(E_1)} = 2\,d_W\sqrt{\frac{m_W^*}{2E_1}} , \tag{2}$$

where m_W^* denotes the effective electron mass in the well. For the energy, we use the value of the first subband E_1, because for the applied doping concentrations the injecting level is always the ground level. The tunneling probability through a rectangular barrier is given by [15]

$$T(E_i) = \frac{1}{1 + \frac{1}{4}\,(x\,+\,x^{-1})^2\,\sinh^2(\kappa\,d_B)} , \tag{3}$$

where $\kappa = \sqrt{2m_B^*\,(V_0 - E_i)}/\hbar$ and

$$x = \sqrt{\frac{m_B^*\,E_i}{m_W^*\,(V_0 - E_i)}} . \tag{4}$$

The escape time $\tau_{esc}(E_i)$ for a single well is determined by the round trip time $\tau_{rt}(E_1)$ divided by the tunneling probability $T(E_i)$ through the barrier [16]

$$\tau_{esc}(E_i) = \frac{\tau_{rt}(E_1)}{T(E_i)} . \tag{5}$$

For the energy in the tunneling probability, we use the value of the subband E_i calculated within the Kronig-Penney model at zero electric field. A schematic diagram of the escape time model for $i = 2$ is shown in Fig. 2.

The frequency of the current oscillations, which is derived from this escape time model, is determined by the inverse of the product of the escape time and the number of periods, which are covered by

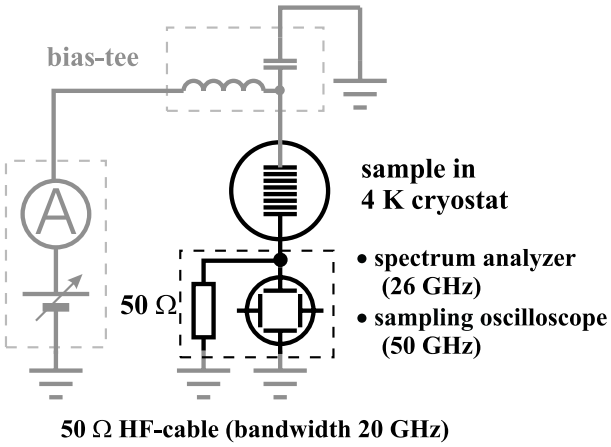

Fig. 1 Schematic diagram of experimental setup for the measurement of the self-sustained current oscillations.

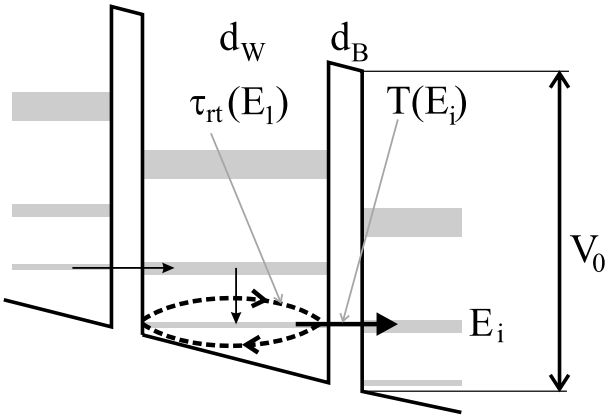

Fig. 2 Schematic diagram of the escape time model with i=2.

the current oscillations. For weakly coupled SLs the recycling motion of the domain boundary includes only about 30% of all periods [2] so that $N_{osc} = 0.3\,N$ and

$$f_{cal} = \frac{1}{N_{osc}\,\tau_{esc}(E_i)} = \frac{T(E_i)}{0.3\,N\,\tau_{rt}(E_1)}\,. \tag{6}$$

4. Measured versus calculated frequencies

We have calculated the oscillation frequencies for all samples listed in Table 1 on the basis of Eq. 6. For the GaAs/AlAs SLs, we used the following parameters, $V_0 = 982$ meV, $m^*_W = 0.067\,m_e$, and $m^*_B = 0.15\,m_e$. The measured versus the calculated frequencies are shown in Fig. 3. For weakly coupled SLs indicated by the solid symbols, the slope of the linear fit in the double-logarithmic plot is 0.92, which is in very good agreement with the expected value of 1. In order to directly compare the calculated with the measured values, we introduce a scaling factor s, which is determined by the ratio of measured and calculated frequencies, i.e. $s = f_i / f_{cal}$. For the weakly coupled SLs in Fig. 3, this factor is about 3 so that the observed frequencies are somewhat larger than the calculated ones. The accuracy of the escape time model is reasonable for weakly coupled SLs, because we use for the calculation of the oscillation frequency in the i^{th} plateau of the I-V characteristic the i^{th} energy level. However, in the high-field domain the electrons tunnel into the $(i+1)^{th}$ level. For that reason the actual oscillation frequency is expected to be somewhat higher than the calculated one. Another simplification is made with regard to the shape of the barriers, since we use rectangular barriers and energy levels calculated within the Kronig-Penney model without any electric field. The variation of the data points between different samples and the consistently higher frequencies in some samples (solid triangles in Fig. 3) could originate from fluctuations of the doping level in the wells. Theoretical calculations show that the oscillation frequency increases by a factor of 5, if the doping level fluctuates by 3% in different wells [17]. Some oscillation frequencies listed in Table 1 were only detected at higher temperatures. Between 5 and 300 K, the frequencies can differ up to a factor of three resulting in some variation of the data points. Finally, another reason for the discrepancy between f_i and f_{cal} could be the actual oscillation mode, which can vary between different SLs [1, 18, 19].

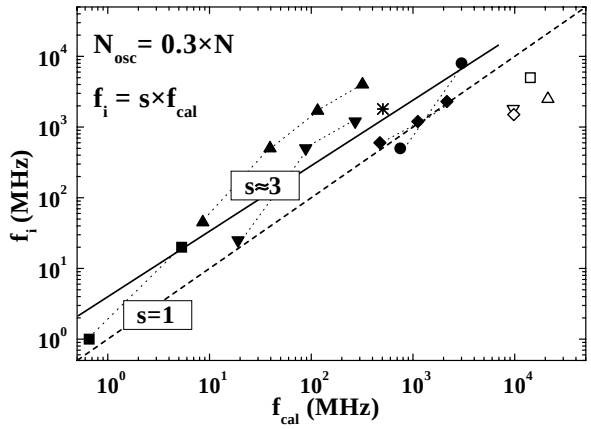

Fig. 3 Measured (f_i) versus calculated (f_{cal}) frequency for the samples listed in Table 1. The same symbols connected with dotted lines indicate oscillations within a single sample in different plateaus. The dashed line indicates the condition $f_{cal} = f_i$, the solid line is a least square fit to the solid data points.

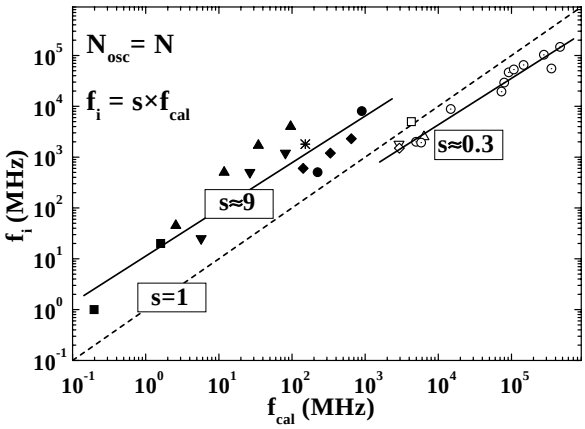

Fig. 4 Measured (f_i) versus calculated (f_{cal}) frequency for the samples listed in Table 1 and the strongly coupled SLs in Ref. [5–7] (dotted circles). Note that we used a different value for N_{osc} in comparison to Fig. 3.

Our simple model appears to be better than the more involved transfer model by Sánchez *et al.* [18]. In this work, the calculated frequency f_2 for the 13.3/2.7 nm GaAs/AlAs SL is about 20 MHz. This value is more than one order of magnitude smaller than the experimental value of 500 MHz. Our model gives 90 MHz.

Note that we did not include the four most strongly coupled SLs (open symbols) in the linear fit of Fig. 3, which have calculated miniband widths of $\Delta_1 = 3.4$–4.5 meV. For these samples, the observed oscillation frequencies are lower than the calculated ones. In order to verify our model for even more strongly coupled SLs, we have also calculated the frequencies of such samples investigated by Schomburg *et al.* [5-7]. In this case, a dipole domain travels through the entire SL. Therefore, we use $N_{osc} = N$ (instead of $N_{osc} = 0.3\ N$) in Eq. 6. The dotted circles in Fig. 4 represent the measured versus calculated frequencies for strongly coupled SLs with miniband widths of $\Delta_1 = 16$–140 meV. The escape time model also works for these samples, since the fit in Fig. 4 has also a slope of about 1. However, the observed oscillation frequencies are now smaller ($s \approx 0.3$) than the calculated ones. We also include all samples from Table 1 in Fig. 4. However, in order to compare the frequencies of weakly SLs with strongly ones, we now assume that the space-charge oscillations cover all periods so that the scaling factor for weakly coupled SLs becomes about 9. There seems to be a fundamental difference between the sequential resonant tunneling (solid symbols) and the miniband transport regime (open symbols). The prefactor changes at miniband widths of a few meV.

5. Summary

In conclusion, we have developed a semiclassical model to predict the frequencies of current self-oscillations in semiconductor SLs from the sample parameters well width, barrier width, effective masses, and band offset. The inverse of the escape time from a single well multiplied by the fraction of the number of SL periods involved in the current oscillation is used as a measure for the oscillation frequency. The escape time is given by the classical round trip time in the well divided by the tunneling

probability through a single barrier. For weakly coupled SLs, where the vertical transport is dominated by sequential resonant tunneling, the agreement between calculated and measured oscillation frequency is as good as can be expected from such a simple model. For more strongly coupled SLs, the measured frequencies are somewhat smaller than the calculated ones. The transition of the prefactor occurs for samples with a miniband width of a few meV, for which the transition between sequential resonant tunneling and miniband transport is expected to occur.

Acknowledgement

The authors would like to thank M. Höricke for assistance in sample growth as well as H. Kostial and E. Wiebicke for sample processing. This work was supported in part by the Deutsche Forschungsgemeinschaft in the framework of Sfb 296.

References

[1] J. Kastrup, R. Hey, K. H. Ploog, H. T. Grahn, L. L. Bonilla, M. Kindelan, M. Moscoso, A. Wacker, and J. Galán, Phys. Rev. B **55**, 2476 (1997).
[2] J. W. Kantelhardt, H. T. Grahn, K. H. Ploog, M. Moscoso, A. Perales, and L. L. Bonilla, Phys. Status Solidi B **204**, 500 (1997).
[3] H. T. Grahn, in *Hot Electrons in Semiconductors, Physics and Devices*, edited by N. Balkan (Clarendon Press, Oxford, 1998), pp. 357–382.
[4] M. Rogozia, R. Hey, H. Kostial, and H. T. Grahn, in *Proceed. of the 26th International Symposium on Compound Semiconductors*, edited by K. H. Ploog, G. Tränkle, and G. Weimann (IOP Publishing, Bristol, 2000), p. 147.
[5] E. Schomburg, T. Blomeier, K. Hofbeck, J. Grenzer, S. Brandl, I. Lingott, A. A. Ignatov, K. F. Renk, D. G. Pavel'ev, Yu. Koschurinov, B. Ya. Melzer, V. M. Ustinov, S. V. Ivanov, A. Zhukov, and P. S. Kop'ev, Phys. Rev. B **58**, 4035 (1998).
[6] E. Schomburg, M. Henini, J. M. Chamberlain, D. P. Steenson, K. Hofbeck, K. F. Renk, and W. Wegscheider, Appl. Phys. Lett. **74**, 2179 (1999).
[7] E. Schomburg, R. Scheuerer, S. Brandl, K. F. Renk, D. G. Pavel'ev, Yu. Koschurinov, V. Ustinov, A. Zhokov, A. Kovsh, and P. S. Kop'ev, Electron. Lett. **35**, 1491 (1999).
[8] S. H. Kwok, T. B. Norris, L. L. Bonilla, J. Galán, J. A. Cuesta, F. C. Martínez, J. M. Molera, H. T. Grahn, K. Ploog, and R. Merlin, Phys. Rev. B **51**, 10171 (1995).
[9] M. Hosoda, H. Mimura, N. Ohtani, K. Tominaga, T. Watanabe, K. Fujiwara, and H. T. Grahn, Appl. Phys. Lett. **69**, 500 (1996).
[10] N. Ohtani, M. Hosoda, and H. T. Grahn, Appl. Phys. Lett. **70**, 375 (1997).
[11] L. L. Bonilla, in *Nonlinear Dynamics and Pattern Formation in Semiconductors and Devices*, edited by F.-J. Niedernostheide (Springer-Verlag, Berlin, 1995), Chap. 1.
[12] A. Wacker, in *Theory of Transport Properties of Semiconductor Nanostructures*, edited by E. Schöll (Chapman and Hall, London, 1998), Chap. 10.
[13] J. B. Gunn, Solid State Commun. **1**, 88 (1963).
[14] M. Shur, *Physics of Semiconductor Devices* (Prentice Hall, Englewood Cliffs, 1990), p. 547.
[15] G. Bastard, *Wave Mechanics Applied to Semiconductor Heterostructures* (Halsted Press, New York, 1988), pp. 229–230.
[16] E. H. Wichmann, *Quantum Physics*, Berkeley Physics Course Vol. 4 (McGraw-Hill, New York, 1971), p. 297.
[17] G. Schwarz, A. Wacker, P. Prengel, E. Schöll, J. Kastrup, H. T. Grahn, and K. H. Ploog, Semicond. Sci. Technol. **11**, 475 (1996).
[18] D. Sánchez, M. Moscoso, L. L. Bonilla, G. Platero, and R. Aguado, Phys. Rev. B **60**, 4489 (1999).
[19] M. Patra, G. Schwarz, and E. Schöll, Phys. Rev. B **57**, 1824 (1998).